

Catastrophe Model for Fast Magnetic Reconnection Onset

P. A. Cassak, M. A. Shay, and J. F. Drake

University of Maryland, College Park, Maryland 20742, USA

(Received 1 February 2005; revised manuscript received 9 June 2005; published 29 November 2005)

A catastrophe model for the onset of fast magnetic reconnection is presented that suggests why plasma systems with magnetic free energy remain apparently stable for long times and then suddenly release their energy. For a given set of plasma parameters there are generally two stable reconnection solutions: a slow (Sweet-Parker) solution and a fast (Alfvénic) Hall reconnection solution. Below a critical resistivity the slow solution disappears and fast reconnection dominates. Scaling arguments predicting the two solutions and the critical resistivity are confirmed with two-fluid simulations.

DOI: [10.1103/PhysRevLett.95.235002](https://doi.org/10.1103/PhysRevLett.95.235002)

PACS numbers: 52.35.Vd, 52.65.-y

Explosive events in plasmas, such as solar eruptions and the sawtooth crash in laboratory fusion devices, are driven by magnetic reconnection. Understanding the mechanism facilitating fast reconnection in high temperature plasma systems has been a long-standing challenge. Sweet-Parker (SP) reconnection [1,2] is far too slow to explain observations and Petschek reconnection requires the invocation of anomalous resistivity, a phenomenon that is at best only poorly understood. A new paradigm has emerged in recent years in which dispersive whistler and kinetic Alfvén waves facilitate fast reconnection by setting up the open Petschek configuration [3–5]. Magnetospheric satellite observations [6] and recent laboratory experiments [7] support this new paradigm.

It is not sufficient, however, to merely explain how fast reconnection can occur. If reconnection were always fast, magnetic stress could never build up in plasma systems such as the solar corona, and the explosive release of magnetic energy seen in nature and the laboratory would never occur. It is critical, therefore, to explain why fast reconnection does not always take place. We show that there are generally two reconnection solutions for a given set of parameters: slow reconnection as predicted by Sweet and Parker, and fast collisionless reconnection facilitated by coupling to dispersive waves in the dissipation region (Hall reconnection). Below a critical resistivity the slow solution disappears. The emerging picture, therefore, is that slow reconnection can dominate the dynamics of a system for long periods of time but the resulting rate of reconnection is so slow that external forces can continue to build up magnetic stresses. When the resistivity η drops below a critical value (or the available free energy crosses a threshold) the system abruptly transitions to fast reconnection and is manifest as a magnetic explosion. Such a model complements earlier ideas that the onset of solar flares, for example, results from the loss of MHD equilibrium [8,9] or more complex “breakout” models [10].

A rather simple argument can be made to motivate why magnetic reconnection is bistable, i.e., has two solutions for a given set of parameters. The Sweet-Parker solution is

valid provided the half width of the current layer δ exceeds the relevant kinetic scale length [11],

$$\frac{\delta}{L} = \sqrt{\frac{\eta c^2}{4\pi c_A L}} > \frac{d_i}{L}, \quad (1)$$

where L is the half length of the SP current sheet, $d_i = c/\omega_{pi}$ is the ion inertial length, ω_{pi} is the ion plasma frequency, and c_A is the Alfvén speed evaluated immediately upstream of the current layer. In writing this equation, we have restricted our attention to the case with no out of plane magnetic (guide) field for simplicity. We take η to be uniform throughout. Equation (1) implies that if a system is undergoing SP reconnection and the resistivity is lowered, SP reconnection will continue as long as Eq. (1) is satisfied.

Conversely, fast reconnection is valid provided the dispersive (whistler or kinetic Alfvén) waves that drive kinetic reconnection [5] are not dissipated. With no guide field, the relevant waves are whistler waves, generated by the Hall term. The dispersion relation for resistive whistler waves is $\omega = k^2 c_A d_i - ik^2 \eta c^2 / 4\pi$. Since both terms scale like k^2 , dissipation can only be neglected if it is small enough at all spatial scales, that is,

$$\frac{\eta c^2}{4\pi} \ll c_A d_i. \quad (2)$$

This can also be written as $\nu_{ei} \ll \Omega_{ce}$, where $\nu_{ei} = \eta n e^2 / m_e$ is the electron-ion collision frequency and $\Omega_{ce} = eB / m_e c$ is the electron cyclotron frequency. This condition is typically easily satisfied in nature but is a significant constraint as we attempt to verify the theory with simulations. Equation (2) implies that if the system is undergoing Hall reconnection and the resistivity is increased, it will stay in the Hall configuration as long as Eq. (2) is satisfied. Putting the two results together, if the resistivity is an intermediate value such that both Eqs. (1) and (2) are satisfied, then either solution is accessible. Therefore, the system is bistable.

We now present estimates of the slow-to-fast (η_{sf}) and fast-to-slow (η_{fs}) resistive transition boundaries of the

bistable regime. We estimate η_{sf} by equating the left and right hand sides of Eq. (1), giving

$$\eta_{sf} \frac{c^2}{4\pi c_A d_i} \sim \frac{d_i}{L}. \quad (3)$$

To estimate η_{fs} , we perform a Sweet-Parker-type scaling analysis [2] that is more precise than the argument used to motivate bistability in Eq. (2). Resistive effects are negligible if the outward magnetic diffusion across the electron current sheet, $\eta c^2/4\pi\delta^2$, is less than the inward convection, v_{in}/δ , where v_{in} is the flow speed into the electron current layer. For Hall reconnection, numerical simulations have shown that δ scales like the electron inertial length $d_e = c/\omega_{pe}$ [3], where $\omega_{pe} = \sqrt{4\pi n e^2/m_e}$ is the electron plasma frequency, and the inflow speed scales like $v_{in} \sim 0.1 c_{Ae}$ [3,12], where c_{Ae} is the electron Alfvén speed based on the magnetic field immediately upstream of the electron current layer. The critical resistivity η_{fs} is found by equating the two:

$$\eta_{fs} \frac{c^2}{4\pi d_e^2} \sim \frac{v_{in}}{d_e} \sim 0.1 \frac{c_{Ae}}{d_e},$$

or, using $c_{Ae} d_e = c_A d_i$,

$$\eta_{fs} \frac{c^2}{4\pi c_A d_i} \sim 0.1, \quad (4)$$

where c_A is evaluated upstream of the *electron* current layer. This is consistent with Eq. (2), but more precise due to the inclusion of the geometry of the layer. The ratio of Eqs. (3) and (4) gives $\eta_{sf}/\eta_{fs} \sim 10d_i/L \ll 1$, which is small because $d_i \ll L$ for most systems of physical interest. Thus, bistability is present over an extensive range of resistivity.

The predictions of this model are amenable to tests using numerical simulations. We use the two-fluid code, F3D, a massively parallel code [13], to perform two-dimensional simulations in a slab geometry of size $L_x \times L_y$. The initial equilibrium is two Harris sheets in a double tearing mode configuration, $\mathbf{B} = \hat{\mathbf{x}}B_0(\tanh[(y + L_y/4)/w_0] - \tanh[(y - L_y/4)/w_0] - 1)$ with $w_0 = 2d_i$ and periodic boundary conditions in both directions. The ions are initially stationary and initial pressure balance is enforced by a nonuniform density. For simplicity, we treat an isothermal plasma. A coherent perturbation to induce reconnection is seeded over the equilibrium magnetic field. The resistivity η is constant and uniform. We use small fourth-order dissipation, $\propto \eta_4 \nabla^4$ with $\eta_4 = 2 \times 10^{-5}$, in all of the equations to damp noise at the grid scale.

The computational domain must be chosen large enough to have a discernible separation of scales between the SP and Hall reconnection rates, but with high enough resolution to distinguish the electron inertial scale. We find that a computational domain of $L_x \times L_y = 409.6d_i \times 204.8d_i$ with a resolution of $\Delta x = \Delta y = 0.1d_i$ and an electron to

ion mass ratio of $m_e = m_i/25$ (i.e., $d_e = 0.2d_i$) is sufficient. A further reduction of Δx and Δy by a factor of 2 does not alter the key results. Since the rate of Hall reconnection is insensitive to the electron mass [4,14,15], we do not expect our results to depend on our particular choice of m_e . For this computational domain, we can estimate η_{sf} and η_{fs} . In evaluating Eq. (3), we use $L \sim L_x/4 = 102.4d_i$. Normalizing lengths to d_i and velocities to $c_{A0} = B_0/\sqrt{4\pi n_0 m_i}$, where n_0 is the initial density far from the sheet, we obtain

$$\eta'_{sf} \equiv \eta_{sf} \frac{c^2}{4\pi c_{A0} d_i} \sim \frac{d_i}{L} \sim 0.01.$$

To evaluate Eq. (4), we use the value of $B \sim 0.3B_0$ upstream of the electron current layer measured in the simulations to evaluate c_A , so

$$\eta'_{fs} \equiv \eta_{fs} \frac{c^2}{4\pi c_{A0} d_i} \sim 0.03.$$

A larger system would produce a greater separation between η'_{sf} and η'_{fs} and would be closer to the parameters of real systems but would be more computationally challenging.

To demonstrate bistability of reconnection with a resistivity in the intermediate region $\eta'_{sf} < \eta' < \eta'_{fs}$, we perform two related sets of simulations. First, we show that a system undergoing Hall reconnection with a resistivity below η'_{fs} continues Hall reconnection for any value of resistivity below this value. We start with a benchmark collisionless ($\eta' = 0$) Hall-MHD simulation that is run from $t = 0$ until the rate of reconnection is steady. The normalized reconnection rate $E' = cE/B_0 c_{A0}$ is shown as a function of island width w as the thick solid line in Fig. 1. The reconnection rate is calculated as the time rate of

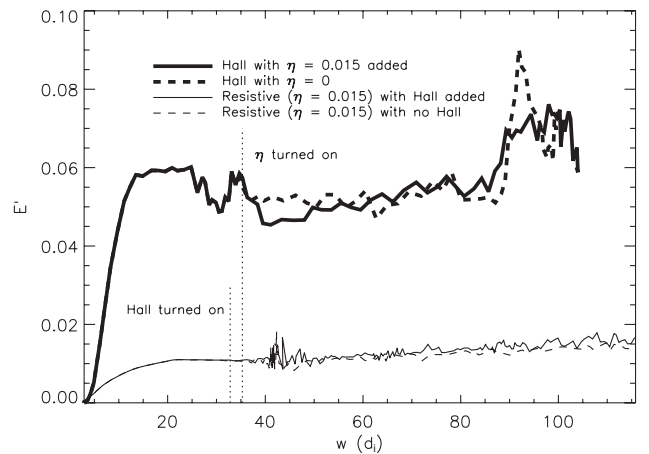


FIG. 1. Normalized reconnection rate, E' , as a function of island width, w , for the two sets of simulations described in the text. The vertical dotted lines show when the added effects were enabled. Note that the final parameters of the two solid line simulations are identical.

change of magnetic flux between the X line and O line. The rate of reconnection jumps to $E' \sim 0.06$ by the time the island width is $10d_i$, after which it remains steady. When $w \sim 35d_i$, we enable a resistivity of $\eta' = 0.015$ (which lies between the predicted values of η'_{sf} and η'_{fs}) and continue the simulation until most of the available magnetic flux has been reconnected. For comparison, the thick dashed line shows the reconnection rate when we maintain $\eta' = 0$. Clearly, the reconnection rate remains nearly unchanged after the inclusion of the resistivity.

For the second set of simulations, we want to show that a system undergoing SP reconnection continues to reconnect at the lower rate for any value of resistivity exceeding η_{sf} . Our computational approach is to disable the Hall and electron inertia terms and evolve the resistive system with a resistivity that exceeds η_{sf} . We then reenables the Hall and electron inertia terms and continue to advance the full equations. This benchmark simulation is performed with $\eta' = 0.015$ (the same value of resistivity as in the run shown in the thick solid line in Fig. 1), and the reconnection rate is again plotted in Fig. 1 as the thin solid line. The reconnection rate remains stationary with $E' \sim 0.01$, a factor of 6 slower than the Hall case even with the Hall and electron inertia terms enabled. For comparison, the thin dashed line in Fig. 1 shows the reconnection rate for a system in which the Hall term is not enabled. Thus, the Hall and the electron inertia terms do not impact the rate of SP reconnection for these parameters.

The out of plane current density, J_z , is shown at late time in Fig. 2 for the runs corresponding to the two solid curves in Fig. 1. The top plot corresponds to the thick solid curve. The current sheet is short and opens wide, as is expected in Hall reconnection [3,16–20]. The bottom plot corresponds to the thin solid curve. The current sheet is long and thin as is expected from the SP theory of resistive reconnection [21–23]. Since the same equations govern the two sets of

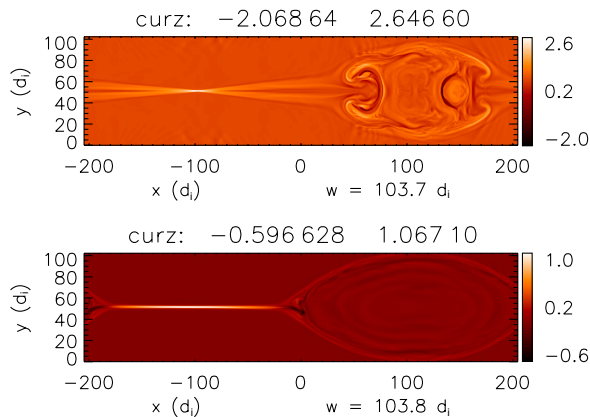


FIG. 2 (color online). Out of plane current density, J_z , for late times from the two solid lines of Fig. 1. The top plot corresponds to the thick solid line (Hall reconnection). The bottom plot corresponds to the thin solid line (SP reconnection).

data and the value of the resistivity is the same, we conclude that the system is bistable.

Next, we test the predictions of η_{sf} and η_{fs} by varying the resistivities of the benchmark Hall and SP reconnection solutions of Fig. 1. For the case of Hall reconnection, corresponding to the thick solid line in Fig. 1, we change η' from 0.0 to 0.010, 0.013, 0.015, 0.0175, 0.020, 0.0225, 0.025, and 0.030 when $w \sim 35d_i$. For the case of SP reconnection, corresponding to the thin solid line in Fig. 1, we change η' from 0.015 to 0.003, 0.007, 0.009, 0.011, 0.013, 0.0175, 0.020, 0.0225, 0.025, and 0.030 when $w \sim 50d_i$ (a short time after the Hall and electron inertia terms have been reenables). The asymptotic reconnection rate is computed as the time averaged reconnection rate once transients have died away.

The results are plotted in Fig. 3(a), with the states starting from Hall reconnection plotted as open circles and the states starting from SP plotted as closed circles. The closed circles reveal that the disappearance of the SP solution occurs abruptly, with η'_{sf} between 0.011 and 0.013. The open circles reveal the disappearance of the Hall reconnection configuration, with η'_{fs} between 0.020 and 0.0225. The error bars are due to random fluctuations in the reconnection rate. The plot is reminiscent of what one would expect of a bifurcation diagram for a system with a cusp catastrophe.

Thus, the numerical simulations confirm that magnetic reconnection is bistable over a range of resistivity consistent with the scaling law predictions of $\eta'_{sf} \sim 0.01$ and $\eta'_{fs} \sim 0.03$. The asymptotic steady state current sheet width

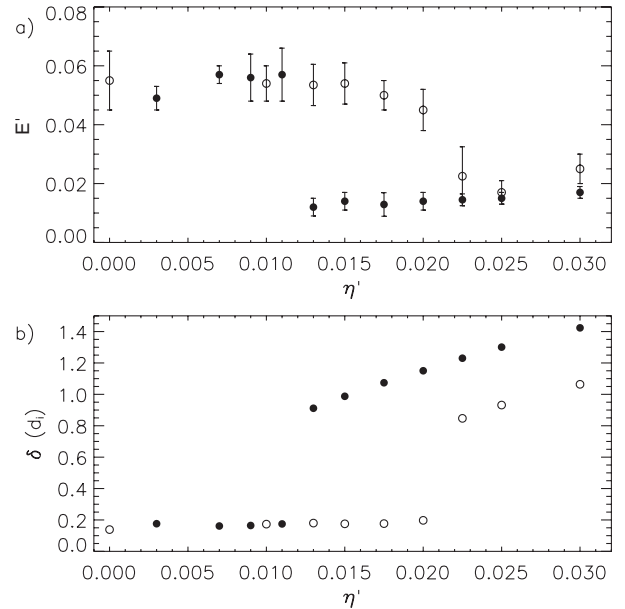


FIG. 3. (a) Steady state normalized reconnection rate, E' , as a function of normalized resistivity, η' for runs analogous to those in Fig. 1 as described in the text. (b) Current sheet width, δ , as a function of η' for the simulations in (a).

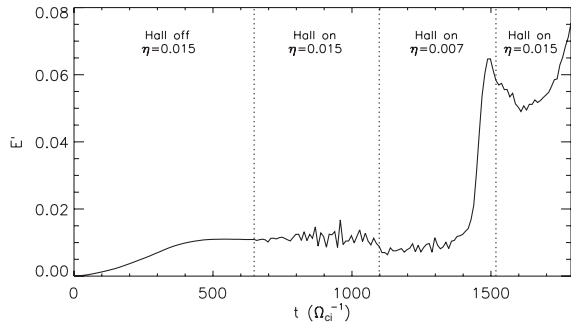


FIG. 4. Normalized reconnection rate, E' , as a function of time t (in units of Ω_{ci}^{-1}) for the simulation which is started at $\eta' = 0.015$, reduced to 0.007, then increased back to 0.015.

δ , calculated as the half width at half maximum of $J_z(y)$ at the X line, is plotted in Fig. 3(b) for each of the runs. As predicted by Eq. (1), the steady state SP current sheet width δ is of order d_i when the resistive reconnection solution ceases to exist, as is shown by the closed circles of Fig. 3(b).

We emphasize that the results presented in Fig. 3, though generated by a specific numerical procedure, are not sensitive to the details of this procedure. To demonstrate this, we show that the key feature of Fig. 3, the boundary where the slow reconnection solution disappears, can be reproduced through a hysteresis-like procedure: in the simulation corresponding to the thin solid line in Fig. 1, we first lower the resistivity from $\eta' = 0.015$ to $\eta' = 0.007$ at $t = 1098\Omega_{ci}^{-1}$ (when the island width is about $w \sim 50d_i$). As expected from Fig. 3 and shown in Fig. 4, the transition from SP to Hall reconnection occurs. We then raise the resistivity back to $\eta' = 0.015$ (the original value) at $t = 1518\Omega_{ci}^{-1}$ (when the island width is about $w \sim 68d_i$). As can be seen in Fig. 4, fast reconnection continues, showing that the system can be in either of two steady states for the same set of parameters.

Finally, we compare our predictions for onset with observations of solar eruptions, for which there is a small guide field. Using values of $n \sim 10^{10} \text{ cm}^{-3}$, $L \sim 10^9 \text{ cm}$, and $B \sim 100 \text{ G}$ [24], Eq. (3) gives a critical resistivity of $\eta_{sf} \sim 10^{-16} \text{ s}$ in cgs units. Using the Spitzer formula, this corresponds to a temperature of $10^2 \text{ eV} \sim 10^6 \text{ K}$, in excellent agreement with the observed coronal temperature. The onset of fast reconnection could therefore take place either as the local coronal temperature or the upstream magnetic field [reflected in c_A in Eq. (1)] increases sufficiently. In the corona, stronger upstream magnetic fields are expected to convect into the X line as reconnection proceeds so the upstream field does increase with time.

The effect of collisionality on the reconnection rate was recently explored in the magnetic reconnection experiment (MRX) [25]. Fast reconnection was only measured when the width of the SP current layer fell below d_i , consistent

with the simulation data presented in Fig. 3(b). In MRX, fast reconnection has been correlated with magnetic turbulence localized in the reconnection layer [26]. Since the present simulations are limited to 2D we cannot address the development of this turbulence and how it might impact our conclusions. An alternative to the present model for fast reconnection onset might involve the onset of strong turbulence and associated anomalous resistivity.

In future work, we will explore whether Eq. (1) holds in the presence of a guide field, for which ρ_s rather than d_i is the relevant kinetic length scale [11]. This may be relevant to the onset of the sawtooth crash in tokamak plasmas.

This work has been supported by NSF Grant No. PHY-0316197 and DOE Grant Nos. ER54197 and ER54784. Computations were carried out at the National Energy Research Scientific Computing Center.

-
- [1] P. A. Sweet, in *Electromagnetic Phenomena in Cosmical Physics*, edited by B. Lehnert (Cambridge University Press, New York, 1958), p. 123.
 - [2] E. N. Parker, *J. Geophys. Res.* **62**, 509 (1957).
 - [3] M. A. Shay *et al.*, *Geophys. Res. Lett.* **26**, 2163 (1999).
 - [4] J. Birn *et al.*, *J. Geophys. Res.* **106**, 3715 (2001).
 - [5] B. N. Rogers *et al.*, *Phys. Rev. Lett.* **87**, 195004 (2001).
 - [6] M. Oieroset *et al.*, *Nature (London)* **412**, 414 (2001).
 - [7] Y. Ren *et al.*, *Phys. Rev. Lett.* **95**, 055003 (2005).
 - [8] M. Hesse and K. Schindler, *Phys. Fluids* **29**, 2484 (1986).
 - [9] J. Lin *et al.*, *New Astron. Rev.* **47**, 53 (2003).
 - [10] S. K. Antiochos *et al.*, *Astrophys. J.* **510**, 485 (1999).
 - [11] D. Biskamp, *Magnetic Reconnection in Plasmas* (Cambridge University Press, Cambridge, UK, 2000).
 - [12] J. D. Huba and L. I. Rudakov, *Phys. Rev. Lett.* **93**, 175003 (2004).
 - [13] M. A. Shay *et al.*, *Phys. Plasmas* **11**, 2199 (2004).
 - [14] M. A. Shay and J. F. Drake, *Geophys. Res. Lett.* **25**, 3759 (1998).
 - [15] M. Hesse *et al.*, *Phys. Plasmas* **6**, 1781 (1999).
 - [16] R. Horiuchi and T. Sato, *Phys. Plasmas* **4**, 277 (1997).
 - [17] P. L. Pritchett, *J. Geophys. Res.* **106**, 3783 (2001).
 - [18] M. M. Kuznetsova *et al.*, *J. Geophys. Res.* **106**, 3799 (2001).
 - [19] M. Hesse *et al.*, *J. Geophys. Res.* **106**, 3721 (2001).
 - [20] F. Porcelli *et al.*, *Plasma Phys. Controlled Fusion* **44**, B389 (2002).
 - [21] D. Biskamp, *Phys. Fluids* **29**, 1520 (1986).
 - [22] D. A. Uzdensky and R. M. Kulsrud, *Phys. Plasmas* **7**, 4018 (2000).
 - [23] B. D. Jemella *et al.*, *Phys. Plasmas* **11**, 5668 (2004).
 - [24] J. A. Miller *et al.*, *J. Geophys. Res.* **102**, 14 631 (1997).
 - [25] M. Yamada *et al.*, in *Magnetic Fields in the Universe*, edited by E. M. de Gouveia Dal Pino, G. Lugones, and A. Lazarian, AIP Conf. Proc. No. 784 (AIP, New York, 2004), p. 27.
 - [26] H. Ji *et al.*, *Phys. Rev. Lett.* **92**, 115001 (2004).